

A New Effective and Efficient Measure of PAPR in OFDM

Ibrahim M. Hussain¹, Imran A. Tasadduq², Abdul Rahim Ahmad³

¹*Department of Computer Engineering, Sir Syed University of Engineering and Technology, Karachi, Pakistan*

²*Department of Computer Engineering, Umm Al-Qura University, Makkah Al-Mukerrimah, Saudi Arabia*

³*Systems Design Engineering, University of Waterloo, Waterloo, Canada*

E-mail: ibrahimh@ssuet.edu.pk, iatasadduq@uqu.edu.sa, arahim@uwaterloo.ca

Received June 28, 2010; revised August 2, 2010; accepted September 3, 2010

Abstract

In multi-carrier wireless OFDM communication systems, a major issue is high peaks in transmitted signals, resulting in problems such as power inefficiency. In this regard, a common practice is to transmit the signal that has the lowest Peak to Average Power Ratio (PAPR). Consequently, some efficient and accurate method of estimating the PAPR of a signal is required. Previous literature in this area suggests a strong relationship between PAPR and Power Variance (PV). As such, PV has been advocated as a good measure of PAPR. However, contrary to what is suggested in the literature, our research shows that often low values of PV do not correspond to low values of PAPR. Hence, PV does not provide a sound basis for comparing and estimating PAPR in OFDM signals. In this paper a novel, effective, and efficient measure of high peaks in OFDM signals is proposed, which is less simpler PAPR. The proposed measure, termed as Partial Power Variance (PPV), exploits the relationship among PAPR, Aperiodic Autocorrelation Co-efficient (AAC), and PV of the transmitted signal. Our results demonstrate that, in comparison to PV, Partial Power Variance is a more efficient as well as a more effective measure of PAPR. In addition, we demonstrate that the computational complexity of PPV is far less than that of PAPR.

Keywords: Aperiodic Autocorrelation Co-Efficient, OFDM, PAPR, Power Variance, Partial Power Variance

1. Introduction

Several communication systems and techniques have been used for transferring data and information reliably at high speed over wireless channel. One such technique is Orthogonal Frequency Division Multiplexing (OFDM) used for high data rate wireless transmission [1]. In OFDM, data bits are transmitted in parallel using various carriers. Although OFDM is a multi-carrier technology, it is very efficacious in mitigating the effects of multipath delay spread over a wireless radio channel. However, a major drawback with OFDM is the high Peak-to-Average Power Ratio (PAPR) of the transmitted signal. The high PAPR mainly results from certain data sequences, such as those containing all zeros or all ones. Such OFDM signals with high peaks result in poor power efficiencies. Appropriate measures should be taken to tackle this problem. Otherwise, the high PAPR signals would substantially limit the usefulness of battery powered equipment such as portable wireless devices. In addition, these high peaks cause problems such as inter-symbol

interference (ISI) and out-of-band radiation. Transmitting high PAPR signals by increasing the operating range of the power amplifier deteriorates the power efficiency of the transmission equipment. Hence, it is imperative to reduce these peaks in the transmission signals. This issue has been addressed by several researchers [2-19]. One widely accepted method for reducing the peaks in OFDM signals is based on using Power Variance (PV) as a measure of PAPR of the signal [2-4]. The computational complexity of PAPR depends on the complexity of the IFFT block, which increases by increasing the number of subcarriers. However, Power Variance is computationally less complex than PAPR for specific range of subcarriers [2-4].

In this paper, we investigate the relationship between the PAPR and the PV of the transmitted OFDM signals. We show that a low value of PV in an OFDM sequence does not always correspond to low value of PAPR and vice versa. Therefore, it would not be generally correct to compare PAPR of different signals by comparing their corresponding PVs. We show that PV is not a good meas-

ure for PAPR and hence, our results contradict the widely accepted premise, as stated in [3,4,20-23]. In addition, the computational complexity of PV is a major drawback, which makes it a poor choice for PAPR performance measurement. Towards this end, we propose a new, effective, and computationally efficient measure, called Partial Power Variance (PPV), for estimating the PAPR. Such approximate and partial computational techniques are quite popular, as well as shown effective in various domains [24,25]. We demonstrate the efficiency of PPV through experimental results.

The rest of the paper is organized as follows. Section 2 introduces OFDM systems. Section 3 describes PAPR as a performance measure for OFDM signals. Section 4 presents various PAPR minimization techniques in OFDM. Section 5 discusses the relationship between AAC, PV and PAPR. Section 6 highlights the computational complexity issues in calculating PV and PAPR. Section 7 proposes PPV as a more efficient and less complex estimator of PAPR. Section 8 concludes the paper with some interesting future research directions.

2. Orthogonal Frequency Division Multiplexing (OFDM)

A typical OFDM system consists of a transmitter and a receiver, as shown in **Figure 1(a)** and **Figure 1(b)** respectively. Such a system works as follows: Serial stream of bits $\{b_0, b_1, b_2, \dots\}$ are encoded using an encoder such that $b_i = 0$ or 1 ; for $i = 0, 1, 2, \dots$. If T_b represents the duration of a single bit then the data rate would be $K = 1/T_b$ bits/second (bps). The serial bit stream at the output of channel encoder is fed into a serial to parallel converter

block that forms a parallel stream. This is achieved by increasing the time period of each bit from T_b to NT_b , where N represents the number of subcarriers used in the OFDM system. These bits are transmitted simultaneously to maintain the same data rate as the original rate of K bps. The number of bits entering a particular branch or subcarrier depends on the mapper (*i.e.* the digital modulation block) which is used after the serial to parallel converter. The number of bits per subcarrier is given by $L = \log_2 M$ where M is the constellation size used by the mapper and depends on the modulation scheme being used. Hence the duration of a symbol per subcarrier is given by $T_s \times N$ where $T_s = L \times T_b$ represents the duration of each subcarrier symbol at the output of the serial to parallel converter which also represents the duration of a single OFDM symbol.

The output of the mapper consists of complex numbers representing the constellation points in a particular modulation scheme. These complex numbers are given by $D = \{d_0, d_1, \dots, d_{N-1}\}$. For Quadrature Phase Shift Keying (QPSK) mapper, the values of d_k can take one of the values from $(1, -1, j, -j)$.

The Inverse Fast Fourier Transform (IFFT) block transforms the discrete complex signal into another discrete complex signal. A typical baseband signal at the output of the IFFT block is given by the following well known Inverse Discrete Fourier Transform (IDFT) Equation [2]:

$$s(q) = \frac{1}{\sqrt{N}} \sum_{k=0}^{N-1} d_k e^{j2\pi kq/N}; k, q = 0, 1, \dots, N-1 \quad (1)$$

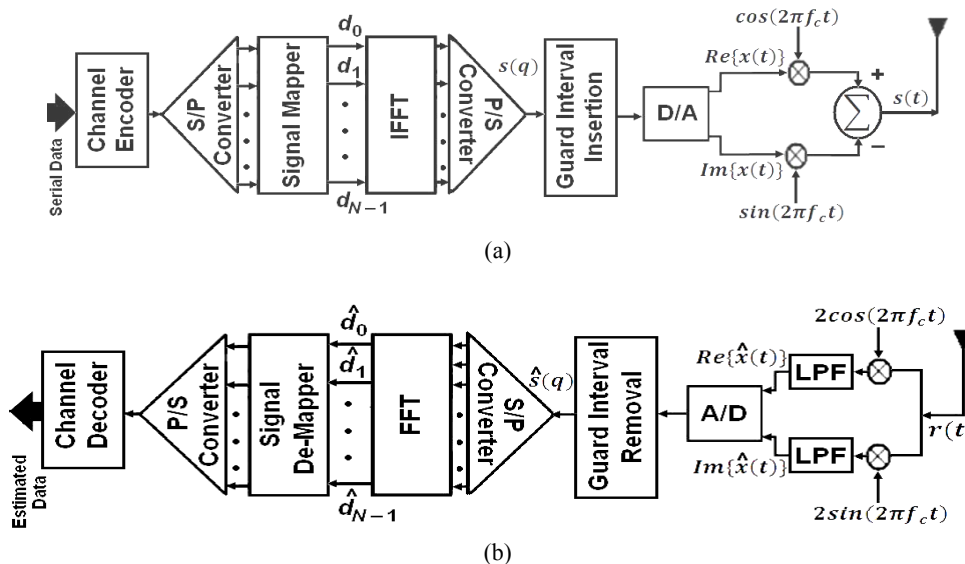


Figure 1. (a) A typical OFDM transmitter; (b) A typical OFDM receiver.

In Equation (1), k indicates the subcarrier index, q is the discrete time index, and d_k represents the complex numbers at the output of the mapper. As indicated by (1), the signal at the output of the IFFT block is the result of summation of various complex sinusoids with varying amplitudes and phases. Hence, the baseband signal given by (1) can be represented as a row vector *i.e.* $S = \{s_0, s_1, \dots, s_{N-1}\}$. The resulting signal is converted into a serial stream using parallel to serial block after which a cyclic prefix or guard interval of length G is appended to it. The discrete-time sequence S which is input to the guard interval block is cyclically extended to form the new symbol sequence which is indicated as

$$S' = \{s_{N-G+1}, s_{N-G+2}, \dots, s_{N-1}, s_0, s_1, \dots, s_{N-1}\}.$$

The cyclically extended discrete-time sequence has new length of $N' = N + G - 1$. This guard interval helps in mitigating the effect of multipath fading in wireless channels. The use of guard interval results in a loss of data throughput as bandwidth is wasted on repeated data. However, in this tradeoff, the loss in data throughput is compensated by significant gains through mitigation in interference. The cyclically extended discrete-time sequence is passed through a digital-to-analog converter to form the baseband OFDM signal. Finally, the baseband OFDM signal is modulated using a carrier frequency for transmission through a wireless channel.

Transmitting a signal through a wireless channel results in convolution of the signal with the impulse response $h(q)$ of the channel. Consequently, the signal is distorted by the additive white Gaussian noise (AWGN) $n(q)$ present in the channel. The convolution between the transmitted signal and channel's impulse response is a circular convolution due to the guard interval. Thus, as seen by channel, the discrete-time sequence S' looks as if s is repeated periodically for all time.

The process of recovering the transmitted data sequence begins with the down conversion of the received signal performed by an IQ detector. The output of the IQ detector is the distorted version of the complex signal $s(t)$, indicated as $\hat{s}(t)$. The signal $\hat{s}(t)$ is passed through an analog-to-digital (A/D) converter to obtain a complex discrete signal $\hat{s}(q)$. Subsequently, the cyclic prefix is discarded and the signal becomes [2]:

$$\hat{s}_q = \sum_{m=0}^{N-1} s_{(q-m)_N} h_m; q = 0, 1, \dots, N-1 \quad (2)$$

where $(q-m)_N$ represents modulo N subtraction. In vector form, \hat{s}_q is represented as $\hat{S} = \{\hat{s}_0, \hat{s}_1, \dots, \hat{s}_{N-1}\}$. After passing the received sequence through the FFT block, an estimate of transmitted complex symbols is obtained which is given by:

$$\hat{d}_k = \frac{1}{\sqrt{N}} \sum_{q=0}^{N-1} \hat{s}_q e^{-j2\pi kq/N}; k = 0, 1, \dots, N-1 \quad (3)$$

After substituting (2) into (3) \hat{d}_k becomes:

$$\hat{d}_k = H_k \times d_k \quad (4)$$

here, H_k represents the transfer function component of the channel and \hat{d}_k is the received subcarrier information at the output of the FFT block. The complex sequence at the output of the FFT block *i.e.* $\hat{D} = \{\hat{d}_0, \hat{d}_1, \dots, \hat{d}_{N-1}\}$ is then passed through the signal de-mapper and parallel-to-serial converter to obtain an estimate of the encoded information. The decoder is then used to arrive at an estimate of the information transmitted.

3. Peak-to-Average Power Ratio (PAPR)

As pointed out in the previous section, the baseband OFDM signal is the result of summation of sinusoidal waves at the output of the IFFT block. At some sample points of these sinusoidal signals, constructive summations may occur, resulting in high peaks in the signal. When transmitting high peak signals through a non-linear power amplifier, distortion occurs within the transmitted signal at the output of the amplifier in the form of ISI and out-of-band radiation. Hence, the influence of high peaks is evident at the output of a non-linear power amplifier but the point of occurrence of these peaks is at the output of an IFFT block. For this reason, the non-linear amplifier is neither used for the analysis throughout the paper nor in simulations being carried out as our main concern revolves around the measurement of these high peaks at the point of occurrence.

One of the widely used measures for the power of these peaks is Peak to Average Power Ratio (PAPR) which is mathematically expressed as:

$$PAPR = \frac{\max\{P(q)\}}{P_{avg}} = \frac{\max_{0 \leq q \leq N-1} |s(q)|^2}{\frac{1}{N} \sum_{q=0}^{N-1} |s(q)|^2} \quad (5)$$

here, $P(q)$ represents the instantaneous power and P_{avg} represents the average power of the OFDM signal. For constant envelope signals, it can be shown that $P_{avg} = N$. In order to simulate such a system, samples of OFDM signals are needed. For better PAPR estimation, oversampling is required to capture these peaks since in normal symbol spaced sampling; some of the peaks might be missed and may result in less accurate PAPR measure. Hence oversampling (1) by a factor of J where ($J > 1$) gives a better PAPR estimation. It has been shown that $J = 4$ is sufficient to capture the peaks [5]. The peak value of an OFDM signal and the corresponding time domain signal differs from one mapper to another (*e.g.* peak in 32-Quadrature Amplitude Modulation (QAM) is different from the peak value in 32-Phase Shift Keying (PSK)).

For all phase shift keying, the maximum peak has the value of N^2 and hence a maximum PAPR of N . **Figure 2** shows all possible OFDM signals for $N = 4$ and BPSK mapper. It can be seen that the maximum normalized absolute peak in such signals is 4 as indicated in the sequences 0000, 1001, 1010 and 1111.

Since the transmitted bits are generated randomly, the transmitted OFDM signals are random in nature and therefore the envelope of an OFDM signal, as given by (1), can be considered a random variable. For large values of N , according to the central limit theorem, the expected amplitudes of OFDM signals follow a Gaussian distribution. In addition, $P(q)$ has a Chi square probability density function with two degrees of freedom [5]. The PAPR performance of a system is usually measured by the Complementary Cumulative Distribution Function (CCDF) curves, a standard way of depicting and describing PAPR related statistics. The CCDF shows the probability of an OFDM sequence exceeding a given PAPR (PAP_0). For PAPR, the lower bound on CCDF for a specific PAPR value (*i.e.*, PAP_0) is given by [7]:

$$\beta = \Pr(PAPR > PAP_0)$$

This results in the following relationship:

$$\beta \geq 1 - (1 - e^{-PAP_0})^N \tag{6}$$

4. Techniques for Minimizing PAPR

The objective is to minimize PAPR as much as possible so as to obtain signals with smaller peaks. Various algorithms and methods have been proposed for reducing PAPR. One simple method for reducing PAPR is direct clipping of high peaks and subsequent filtering of the signal [7,8]. In addition, various modulation schemes are used for efficient transmission of signals such as Continuous Phase Modulation (CPM) [9,10].

Recently, constellation and shaping methods have

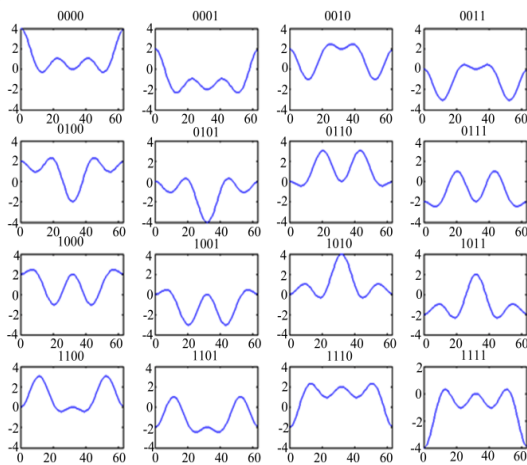


Figure 2. Peak values in OFDM signals for $N = 4$ by using BPSK mapper.

been used to reduce PAPR. In these methods, a mapping between the original complex numbers and the finally transmitted complex numbers takes place based on an algorithm or a coding technique. One such method is the trellis shaping method using a metric which is based on the Viterbi algorithm [11]. One of the variants of this method uses a metric-based symbol predistortion algorithm resulting in some implementation complexity [12]. Another promising technique for reducing PAPR involves scrambling the incoming OFDM sequence using some rotation vectors resulting in multiple signals that represent the same original information. Among these signals, the signal with the lowest PAPR is transmitted. Examples of such methods are Selected Mapping (SLM) [13-15] and Partial Transmit Sequence (PTS) [16,17]. In SLM, shown in **Figure 3(a)**, from a single OFDM sequence of length N , U sequences are generated that represent the original information or OFDM sequence. The sequence having lowest PAPR value is transmitted. These sequences are generated by multiplying the original OFDM sequence with U different factors. These factors are given in vector form as $B^{(i)} = [b_0^{(i)}, b_1^{(i)}, \dots, b_{N-1}^{(i)}]$ where $i = 1$ to U represents the indices of these factors. After multiplying these factors by the original OFDM sequence D , we get $X^{(i)} = [d_0 b_0^{(i)}, d_1 b_1^{(i)}, \dots, d_{N-1} b_{N-1}^{(i)}]$. These factors are phase rotations selected appropriately such that multiplying a complex number by these factors

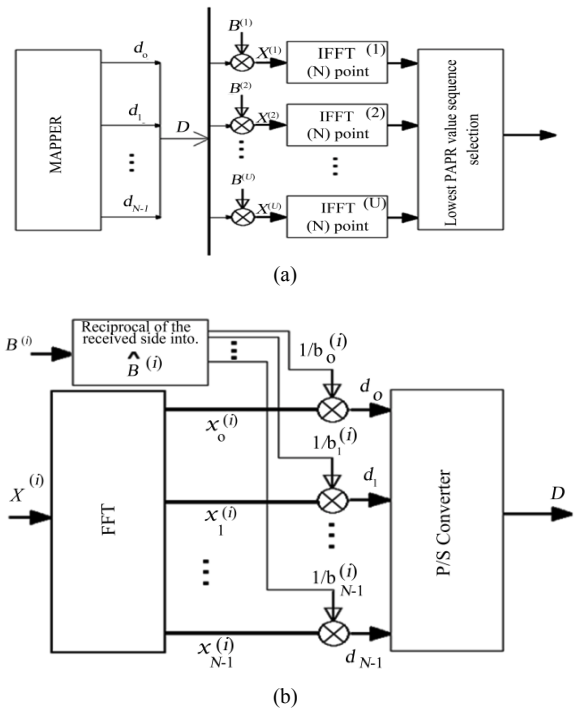


Figure 3. The SLM method (a) at the transmitter and (b) at the receiver.

results in rotation of that complex number to another complex number representing a different point in the constellation. Hence, $b_n^{(i)} = e^{-j\theta_n^{(i)}}$ where $\theta_n^{(i)} \in [0, 2\pi)$.

At the receiver end as shown in **Figure 3(b)**, the original OFDM sequence is recovered by multiplying the received sequence by the reciprocal of the vector being used at the transmitter end. Hence, in SLM, it is essential to transmit the rotational vector $B^{(i)}$ as side information to recover the original sequence.

On the other hand, in PTS method, as shown in **Figure 4**, the original OFDM sequence D is first partitioned into H disjoint sub-sequences. The length of each sub-sequence is still N but padded with zeros. Each sub-sequence is fed into a separate IFFT block of length N each. Hence, there are H number of IFFT blocks. The set of complex numbers at the output of each IFFT block is multiplied by a factor belonging to one of the rotation factors as indicated in SLM technique. These factors are optimized in such a manner that the PAPR of the combined sub-sequences are reduced. After multiplying by the factors, the complex numbers from all the IFFT blocks are added together carrier-wise, resulting in a final sequence. This final sequence has lower PAPR than the original one.

Many other proposed algorithms tackle different parameters for reducing the PAPR indirectly. One such method is the Aperiodic Autocorrelation Coefficient (AAC) of the transmitted OFDM signals in which PAPR reduction is achieved using selective scrambling of the transmitted sequence, generating a number of statistically independent sequences [2]. A Selective Function (SF) is computed for every sequence and the sequence with the lowest SF, which also corresponds to the lowest PAPR, is transmitted.

Another factor that plays an important role in reducing

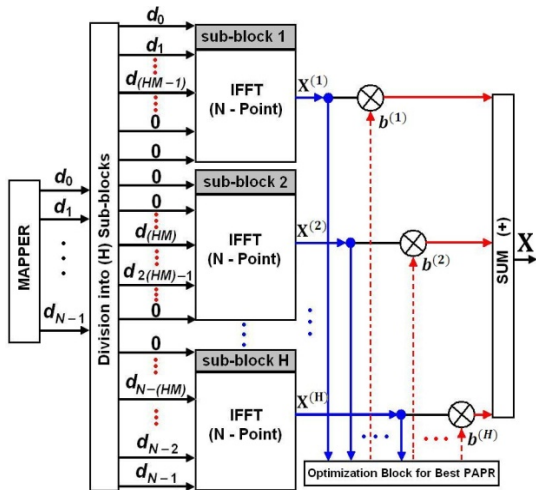


Figure 4. PTS method.

PAPR is the Power Variance (PV) of an OFDM sequence. It is indicated in the literature that there exists a strong relationship among AAC, PV and PAPR [2-4,20-23,26]. In the next section, we study this relationship in OFDM signals.

5. PV and Aperiodic Autocorrelation Coefficients

For a complex envelope signal given by (1), the instantaneous power is given as:

$$P(q) = (q)S^*(q) \tag{7}$$

where ‘*’ denotes conjugate of a complex signal. By combining (1) and (7) we get:

$$P(q) = \frac{1}{N} \sum_{k=0}^{N-1} \sum_{p=0}^{N-1} d_k e^{j2\pi kq/N} d_p^* e^{-j2\pi pq/N} \tag{8}$$

Since the subcarriers in the OFDM signal are orthogonal, they satisfy the following condition [2]:

$$\sum_{q=0}^{N-1} \Phi(i, q) \Phi^*(j, q) = \begin{cases} 0, & i \neq j \\ N, & i = j \end{cases} \tag{9}$$

such that,

$$\Phi = \begin{bmatrix} 1 & 1 & \dots & 1 \\ 1 & e^{j2\pi/N} & \dots & e^{j2(N-1)\pi/N} \\ \vdots & \vdots & \ddots & \vdots \\ 1 & e^{j2(N-1)\pi/N} & \dots & e^{j2(N-1)^2\pi/N} \end{bmatrix} \tag{10}$$

By simple manipulation of (8) and using the orthogonality property of the subcarriers given by (9), the instantaneous power can be expressed as:

$$P(q) = \frac{1}{N} \left[R_0 + \sum_{i=1}^{N-1} R_i e^{-j2\pi iq/N} \sum_{i=1}^{N-1} R_i^* e^{j2\pi iq/N} \right] \tag{11}$$

where R_i is called the i th Aperiodic Autocorrelation Co-efficient of the complex OFDM sequence D and given as [3]:

$$R_i = \sum_{k=0}^{N-1-i} d_k d_{k+i}^* ; 0 \leq i \leq N-1 \tag{12}$$

Note that for $i = 0$, (12) becomes $R_0 = \sum_{k=0}^{N-1} |d_k|^2 = P_{avg}$.

in case of a constant envelope mapper, $P_{avg} = N$. By combining (11) and (12) then dividing by P_{avg} , we get the normalized instantaneous power $\gamma(q)$ given below:

$$\gamma(q) = \frac{P(q)}{P_{avg}} = \frac{1}{NP_{avg}} \left[N + \sum_{i=1}^{N-1} R_i \left\{ \cos\left(\frac{2\pi iq}{N}\right) - j \sin\left(\frac{2\pi iq}{N}\right) \right\} + \sum_{i=1}^{N-1} R_i^* \left\{ \cos\left(\frac{2\pi iq}{N}\right) + j \sin\left(\frac{2\pi iq}{N}\right) \right\} \right]$$

hence, $\gamma(q)$ is given by:

$$\gamma(q) = \frac{1}{NP_{avg}} \left[N + 2 \sum_{i=1}^{N-1} \text{Re}\{R_i\} \cos\left(\frac{2\pi iq}{N}\right) - 2 \sum_{i=1}^{N-1} \text{Im}\{R_i\} \sin\left(\frac{2\pi iq}{N}\right) \right] \quad (13)$$

In compact form, (13) can be reduced into:

$$\gamma(q) = \frac{1}{NP_{avg}} \left[R_0 + 2 \sum_{i=1}^{N-1} |R_i| \cos\left(\frac{2\pi iq}{N} + \tan^{-1}\left(\frac{\text{Im}\{R_i^*\}}{\text{Re}\{R_i\}}\right)\right) \right] \quad (14)$$

Using Chebyshev polynomials, an upper bound on (14) is given by [19]:

$$\gamma(q) \leq \Gamma = \frac{1}{NP_{avg}} \left[R_0 + 2 \sum_{i=1}^{N-1} |R_i| \right] \quad (15)$$

By taking the difference between the instantaneous power and the average power, *i.e.* $\Delta P(q) = P(q) - P_{avg}$, we get the Power Variance of OFDM signal using the following expression:

$$PV = \frac{1}{N} \sum_{q=0}^{N-1} [\Delta P(q)]^2$$

which can be further expanded using trigonometric properties into the following expression:

$$PV = \frac{1}{N} \left[\frac{4}{N^2} \sum_{i=1}^{N-1} \sum_{m=1}^{N-1} |R_i| |R_m| \times \left[\sum_{q=1}^{N-1} \cos\left(\frac{2\pi iq}{N} + \varphi_i\right) \cos\left(\frac{2\pi mq}{N} + \varphi_m\right) - N(P_{avg} - 1)^2 \right] \right] \quad (16)$$

Hence, an upper limit on (16) becomes:

$$PV \leq PV_{norm} = \sum_{i=0}^{N-1} |R_i|^2 \quad (17)$$

here, PV_{norm} is the normalized power variance. It can be observed from (11-15) that $P(q)$, $\gamma(q)$ and Γ are all functions of AAC. Low values of $|R_i|$ correspond to low instantaneous power and hence low values of Γ . Based on this assessment, some authors use (15) as a parameter for measuring and comparing PAPR values of OFDM sequences. In contrast, other authors show that PAPR analysis based on (14) and (15) gives misleading results [19]. Through an example, they show that sequences exist that have low PAPR values but high Γ values and vice versa. They conclude that Γ cannot serve as parameters for PAPR comparison of sequences and hence Γ is not a good measure for PAPR. In addition, many authors concluded that PV is also a good measure of PAPR [2-4,20-23]. However, in subsequent paragraphs, we show that this is not always the case.

Figures 5 and 6 show normalized PAPR and PV values respectively for different sets of 300 randomly generated OFDM sequences when eight subcarriers are used. Apparently, these figures suggest that PV is a good measure

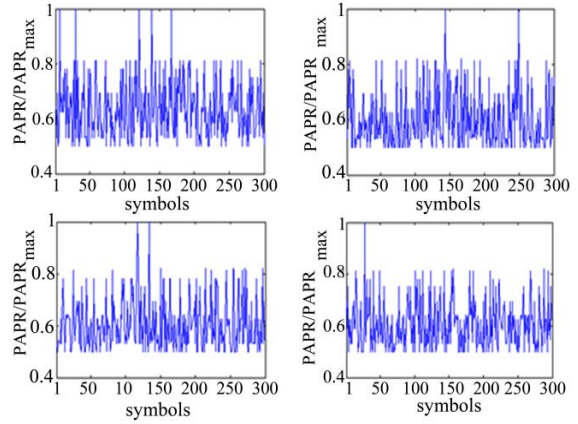


Figure 5. Normalized PAPR for randomly generated OFDM sequences with 8 subcarriers.

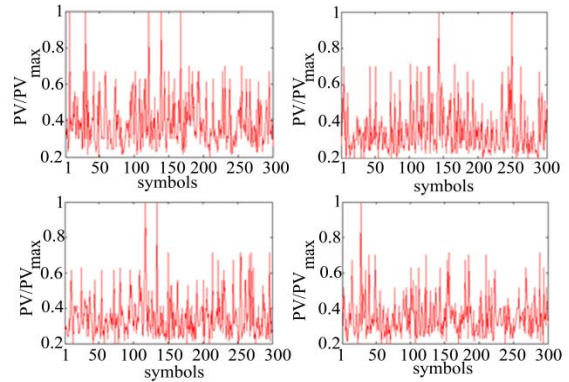


Figure 6. Normalized PV for randomly generated OFDM sequences with 8 subcarriers.

of PAPR as the pattern of both the figures for the same set of symbols is almost the same. Hence, many authors concluded that PV is a good measure for PAPR [2-4,20-23]. However, we here demonstrate that this observation is misleading because not all low PAPR sequences have low PV and vice versa. To refute this assertion, we investigate the relation between PV and PAPR given as [4,5]:

$$Q\left(\frac{PAPR-1}{\sqrt{PV}}\right) + Q\left(\frac{1}{\sqrt{PV}}\right) = \beta \quad (18)$$

where $Q(\cdot)$ is the complementary error function and β denotes $Pr(P(q) \leq P(q)_{max})$ which is given by (6). Figure 7 shows a plot of (18) for selective values of PAPR for 256 subcarriers with $\beta = 0.7434$. Two aspects in this **Figure 7** are noteworthy. First, for a particular value of PAPR, there are two values of PV. For instance, at PAPR = 6.5 dB, the values of PV are 35 and 93.37. Second, PV does not vary in proportion to PAPR. For instance, at PAPR = 6dB, one of the values of PV is 79.89 whereas at PAPR = 7dB, one of the values of PV is 44.31, *i.e.* an in-

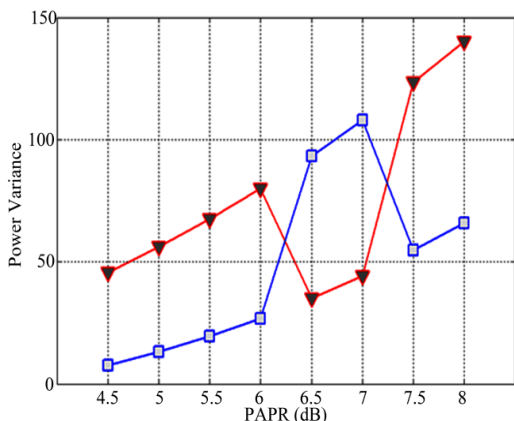


Figure 7. Relationship between PAPR and PV for $\beta = 0.7434$ with 256 subcarriers.

crease in PAPR does not always correspond to an increase in PV. It shows that PV cannot always constitute a basis for comparison of PAPR between two sequences.

Hence, PV cannot be considered a reliable measure for PAPR. In addition, to emphasize our assessment of relationship between PV and PAPR, CCDF plots are used for PAPR measure based on PV using SLM and PTS techniques.

In the first simulation experiment, CCDF curves are plotted for 50,000 randomly generated OFDM sequences using SLM technique where $U = 4, 16$ and 64 as shown in **Figure 8**. In this approach, U different sequences are generated from a single OFDM sequence D using randomly generated phase rotation factors. The sequences having the lowest PV and the lowest PAPR are selected for transmission. In short, the selection decision for transmitting a sequence is based on both the lowest PV and the lowest PAPR. This simulation gives two sets of CCDF curves, as shown in **Figure 8**. It is clear that the reduction in PAPR based on PV is not the same as the one based on PAPR. For instance at CCDF = 0.001, when $U = 64$, the PAPR reduction using a PV-based decision is approximately 2dB while the PAPR reduction based on PAPR itself is around 3.8dB . A difference of almost 2dB is evident between the two transmission decisions. This difference in PAPR reduction is sufficient to show that PV is not a good and reliable measure for the purposes of PAPR reduction.

For the second simulation experiment, CCDF curves are plotted for 50,000 randomly generated OFDM sequences using PTS technique using 256 subcarriers and $H = 16$, shown in **Figure 9**. As it is the case in SLM, two curves are generated for both PV- and PAPR-based transmission decisions. A PAPR reduction of 2dB is achieved in case of PV-based decision whereas a reduction of 3.5dB is achieved in case of PAPR-based decision. Once again, the difference in PAPR performance be-

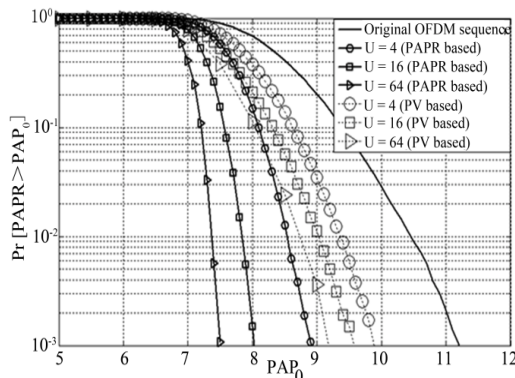


Figure 8. CCDF curves for SLM based on PAPR and PV for various values of U .

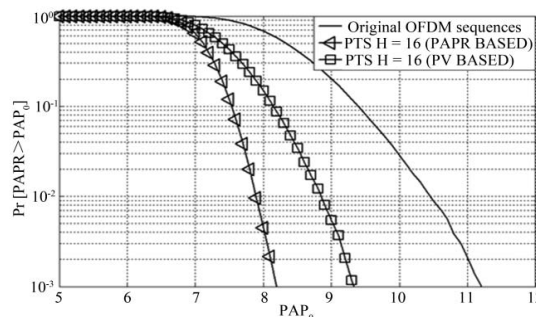


Figure 9. CCDF curves for PTS technique based on PAPR and PV for $H = 16$.

tween PV-based and PAPR-based transmission decisions is significant and obvious. All these results suggest that low values of PV do not always correspond to low PAPR values and vice versa. Consequently, PV is not a reliable measure of PAPR and it cannot be used as a parameter for OFDM sequence selection in both SLM and PTS techniques. Since OFDM sequences follow a random process, it is difficult to tell the range of PAPR values or sequences that correspond to high PV values and vice versa.

It can also be noted that for a particular number of subcarriers N , the values of β vary with PAPR values. Although theoretically PAPR, PV and β can take any value, as indicated by (18), the actual values of these three parameters are finite and specific for a given number of subcarriers. For instance, through simulation we generate all possible OFDM symbols for 16 subcarriers using BPSK mapper and plot their corresponding PAPR values against PV values as shown in **Figure 10**. The total number of possible OFDM symbols is 65,536. The maximum and minimum PAPR values are 16 and 1.7071 respectively and the corresponding PV values for these PAPR values are 1240 and 24 respectively. Note that the plot is discontinuous through PAPR axis because the

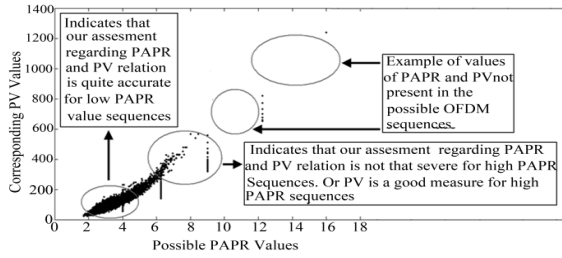


Figure 10. PV versus PAPR values for OFDM sequences with 16 subcarriers and BPSK mapper.

OFDM symbols have finite and specific values of PAPR, as mentioned earlier.

It is interesting to note that our assessment regarding the relation between PV and PAPR is more pronounced for low values of PAPR than high values of PAPR (*i.e.* more concentration of points in the lower region of PAPR). It can be seen that for a single PAPR value in the lower range (approximately from 2dB to 5dB), there are more than one corresponding PV value. Similarly, for a single value of PV (approximately from 24 to 300), there are more than one corresponding PAPR value. Again, this plot is only possible for small number of subcarriers. For high number of subcarriers, it is difficult to find the distribution of PAPR and PV values for all possible OFDM sequences.

6. Computational Complexity of PV

SLM algorithm based on PAPR comparison has moderate complexity. The main complexity is based on the computation of IFFT operation. This complexity increases as U increases. Hence, IFFT has to be computed for every sequence (*i.e.* U times) before transmitting the final selected sequence. Similarly, when evaluating PV, Equation (17) needs to be evaluated for every sequence (*i.e.* U times) before transmitting the final selected sequence. So, it would be interesting to compare the complexity associated with computing PAPR with the complexity in evaluating PV.

The complexity expressions in terms of complex additions and multiplications for evaluating IFFT, and therefore PAPR, are shown in **Table 1** [28]. Similarly it could easily be shown that the complexity for evaluating Equation (17) in terms of both complex additions and multiplications is given as:

$$\left. \begin{aligned} \text{Complex Additions} &= \frac{N(N-1)-2}{2} \\ \text{Complex Multiplications} &= (N-1)\left(\frac{N}{2}+1\right) \end{aligned} \right\} \quad (19)$$

Table 1. Computational complexity of various parameters.

Expression	Complex Additions	Complex Multiplications
IFFT	$JN(\log_2 JN)$	$JN(\log_2 JN)/2$
IFFT and PAPR	$JN(\log_2 JN)$	$(JN(\log_2 JN)/2) + JN$
PV	$(N(N-1)-2)/2$	$(N-1)((N/2)+1)$
PPV	$(B(2N-B-1)-2)/2$	$(B(2N-B-1)/2) + B$

Table 2. Computational complexity of various parameters for different subcarriers.

N	Complex Additions				
	PAPR ($J=1$)	PAPR ($J=4$)	PV	PPV (B)	PPV ($B=1$)
4	8	64	5	4 (2)	2
8	24	160	27	21 (4)	6
16	64	384	119	91 (8)	14
32	160	896	495	219 (8)	30
64	384	2048	2015	475 (8)	62
128	896	4608	8127	1911 (16)	126
256	2048	10240	32639	3959 (16)	254
N	Complex Multiplications				
	PAPR ($J=1$)	PAPR ($J=4$)	PV	PPV (B)	PPV ($B=1$)
4	4	32	9	7 (2)	4
8	12	80	35	26 (4)	8
16	32	192	135	100 (8)	16
32	80	448	527	228 (8)	32
64	192	1024	2079	448 (8)	64
128	448	2304	8255	1928 (16)	128
256	1024	5120	32895	3976 (16)	256

The computational complexity for both PAPR and PV for different values of N is presented in **Table 2**. Note that, for comparison purposes, PAPR complexity is also evaluated when oversampling OFDM signals by a factor of 4. It is clear that the computational complexity of PV is lower than that of PAPR only for very small values of N (*i.e.* $N=2$ and 4). For large values of N , the computational complexity of PV is far greater than that of PAPR complexity even when $J=4$. Hence, PV-based selection becomes impractical for large values of N . This is another disadvantage of using PV as a selection criterion in SLM or PTS techniques, pronouncing the need for an efficient measure of PAPR. In the next section, we propose one such measure of PAPR

7. AAC-SLM Algorithm and Partial Power Variance (PPV)

In this section, we introduce a new parameter called Par-

tial Power Variance (PPV) that can be effective in reducing PAPR. Indeed, such Soft Computing tools and approximate, but effective and efficient, computational techniques are rapidly gaining popularity in subjective and complex application domains [24,25]. We show that PPV is not only effective but also computationally efficient than both PV and PAPR. Towards this end, we also propose an algorithm for minimizing PAPR. The proposed algorithm is modeled on SLM technique and we call it AAC-SLM. As indicated by (17), the normalized PV expression consists of $N - 1$ aperiodic autocorrelation coefficients. The objective of AAC-SLM algorithm is to investigate these coefficients (*i.e.* R_1, R_2, \dots, R_{N-1}) individually and find their contribution in reducing PAPR. For QPSK mapper, the proposed algorithm involves the following steps. From a single OFDM sequence, $(N-1)$ different sequences are generated by reducing $|R_i|$ of the sequence to its minimum possible values of 0 (for even i) and 1 (for odd i) where $i = 1, 2, \dots, N-1$. These sequences represented by Y_1, Y_2, \dots, Y_{N-1} have the following property: the generated sequence Y_i is the result of minimizing $|R_i|$ of the original OFDM sequence to its minimum value (*i.e.* either 0 or 1 depending on i). Hence, for each new sequence, only its respective $|R_i|$ is minimized while other $|R_i|$'s for that sequence may not have minimum value. For example, a sequence generated by minimizing $|R_3|$ *i.e.* Y_3 may or may not have minimum values of other $|R_i|$, *i.e.* $|R_1|, |R_2|, |R_4|, \dots$ etc. From these sequences, the one with the lowest PAPR is transmitted. The method for reducing the coefficients to their minimum values is given in the Appendix.

The CCDF curves for AAC-SLM algorithm using 256 subcarriers and 100,000 randomly generated OFDM sequences are shown in **Figure 11**. It is clear that a maximum reduction of 3.8 dB is achieved when all sequences from Y_1 through Y_{255} are included. The sequence with the lowest PAPR is selected. Further, when reducing the number of sequences to 64 (*i.e.* Y_1, Y_2, \dots, Y_{64}) and selecting the one with lowest PAPR, a negligible degradation in PAPR occurs. This suggests that the higher order sequences Y_{65} through Y_{255} only have a marginal and negligible contribution in reducing PAPR. Similarly, when considering only Y_1 and Y_2 , a PAPR reduction of 3.2dB is achieved. In fact, only by reducing the first AAC (*i.e.* Y_1 only), almost 3dB reduction is achieved in PAPR performance. In other words, all the generated sequences in the AAC-SLM algorithm other than Y_1 have a minimal contribution in PAPR reduction. It follows that all AAC in the PV expression have a minimal contribution in PAPR reduction except for $|R_1|$.

Based on the previous observations, **Figure 8** is re-

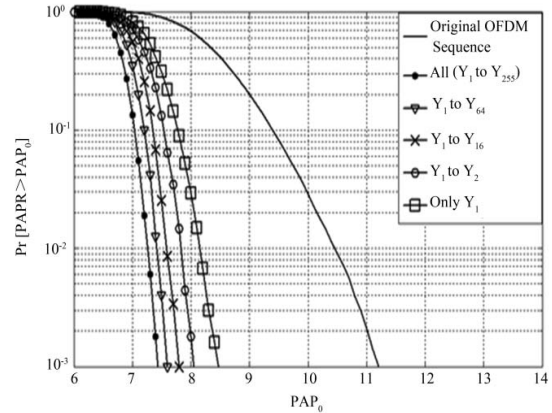


Figure 11. AAC-SLM with 256 subcarriers.

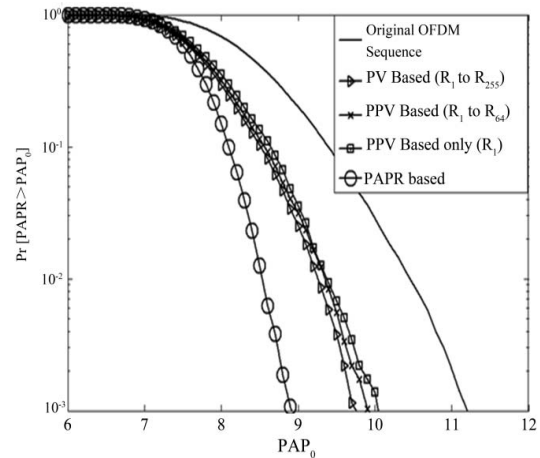


Figure 12. PPV in PAPR reduction for different values of B with $N = 256$.

plotted for $U = 4$, shown in **Figure 12**. Around 100,000 OFDM symbols are randomly generated to carry out this experiment. Similar to **Figure 8**, CCDF curves for both PV- and PAPR-based decision are shown in **Figure 12**. The two additional CCDF curves are a result of making the transmission decision based on PPV, where PPV is the truncated version of the PV expression given by (17). The first curve is generated when the decision is based only on the first 64 AAC (R_1, R_2, \dots, R_{64}) in (17) instead of using the whole expression for PV. Hence in this case, From **Figure 12** it is clear that a negligible degradation in PAPR performance results using this truncated expression. In fact, when a single AAC is used *i.e.* $PPV = |R_1|^2$, a degradation of only 0.2dB occurs from the PV-based CCDF curve. These results also support our earlier observations for the efficacy of the AAC-SLM algorithm. In other words, we can say that AAC terms in PV expression do not contribute in reducing PAPR significantly except for the first term *i.e.* R_1 that has the maximum contribution in reducing PAPR. In short, we can use PPV instead of PV while achieving almost the same

PAPR reduction.

In addition, the computational complexity of PPV is less than both PV and PAPR. To compare the computational complexities of the PV- and PPV-based decisions, we write a general expression for PPV as follows:

$$PPV_B = \sum_{i=1}^B |R_i|^2 \quad (20)$$

where B indicates the number of AAC terms included in the PPV expression. Note that when $B = N - 1$, PPV expression becomes PV. In terms of B , the complexity of PPV is given below (and also shown in Table 1):

$$\left. \begin{aligned} \text{Complex Additions} &= \frac{B(2N - B - 1) - 2}{2} \\ \text{Complex Multip.} &= \frac{B(2N - B - 1)}{2} + B \end{aligned} \right\} \quad (21)$$

In case of $B = 1$, the complexity reduces to $N - 2$ and N complex additions and multiplications, respectively. This shows a considerable reduction in computational complexity when PPV is used for transmission decision instead of PV or even PAPR itself. The reduction in computational complexity for different values of B is shown in **Table 2**. Once again, it can be seen that the maximum reduction in complexity is achieved when $B = 1$. For instance, in case of 256 subcarriers, the number of complex additions in PAPR (with $J = 1$) is 2048, whereas in case of PPV_1 it reduces to 254, a reduction by a factor of nearly 8. The computational complexity is decreased considerably compared with IFFT complexity. Hence PPV is faster to implement both in hardware using digital signal processing techniques and software than IFFT.

8. Conclusions

In this paper, we have established that PV is not a good measure of power efficiency as has been claimed in the literature. Our results clearly show that using PV as the power efficiency measure gives misleading results. Further, we show that PV is computationally more complex than PAPR and hence cannot be used as a power efficiency measure for OFDM. In addition, we have developed a new, effective and efficient measure for power efficiency called PPV which is computationally less complex than PAPR. The amount of reduction achieved in terms of complex additions and multiplications for a 256-subcarrier system is more than 8 times as compared to PV and 3.5 times as compared to PAPR in order to achieve the best power efficiency. In fact, based upon the flavor used for PPV, the reduction in complexity may go down as low as 40 times as compared to PAPR at a nominal degradation in power efficiency. Hence, PPV is a more useful, realistic and cost-effective measure for power

efficiency of OFDM signals. In this paper, we demonstrated the efficacy of the new measure by applying it on PTS and SLM techniques. The proposed measure can also be applied on other established algorithms to decrease the computational complexity. Further, the performance of the new measure can also be tested for more practical systems where the number of subcarriers may go beyond 2048.

In this paper the bit error rate (BER) performance of PPV is not discussed as the main objective was to investigate the PAPR performance of PPV. As a future work, it would be interesting to find out the BER performance of PPV both in AWGN and multipath fading channels.

9. References

- [1] Special Issue on 4G Mobile Communications: "Toward Open Wireless Architecture," *IEEE Wireless Communications*, Vol. 11, No. 2, April, 2004.
- [2] P. Van Eetvelt, G. Wade and M. Tomlinson, "Peak to Average Power Reduction for OFDM Schemes by Selective Scrambling," *Electronics Letters*, Vol. 32, No. 21, October 1996, pp. 1963-1964.
- [3] H. Nikookar and R. Prasad, "Weighted Multicarrier Modulation for Peak-to-Average Power Reduction," *IEICE Transactions on Communications*, Vol. E83-B, August 2000, pp. 1396-1404.
- [4] H. Nikookar and Knut Sverre Lidsheim, "Random Phase Updating Algorithm for OFDM Transmission with Low PAPR," *IEEE Transactions on Broadcasting*, Vol. 48, No. 2, June 2002, pp. 123 - 128.
- [5] C. Tellambura, "Use of M-sequences for OFDM Peak-to-average Power Ratio Reduction," *IEEE Electronics Letters*, Vol. 33, No. 15, July 1999, pp. 1300-1301.
- [6] C. Tellambura, "Computation of the Continuous-Time PAR of an OFDM Signal with BPSK Subcarriers," *IEEE Communications Letters*, Vol. 5, No. 5, May 2001, pp. 185-187.
- [7] K. Y. Xue, H. W. Yang and S. L. Su, "The Clipping Noise and PAPR in the OFDM System," *Proceedings of WRI International Conference on Communications and Mobile Computing*, Vol. 1, Yunnan, January 2009, pp. 265-269.
- [8] H. Gacanin and F. Adachi, "PAPR Advantage of Amplitude Clipped OFDM/TDM," *IEICE Transactions on Communications*, Vol. E91-B, No. 3, March 2008, pp. 931-934.
- [9] I. A. Tasadduq and R. K. Rao, "OFDM-CPM Signals for Wireless Communications," *Canadian Journal of Electrical & Computer Engineering*, Vol. 28, No. 1, January 2003, pp. 19-25.
- [10] I. A. Tasadduq and R. K. Rao, "PAPR Reduction of OFDM-CPM System Using Multi-Amplitude CPM Signals," *Proceedings of 21st Biennial Symposium on Communications*, Kingston, June 2002, pp. 225-229.

- [11] H. Ochiai, "A Novel Trellis-shaping Design with Both Peak and Average Power Reduction for OFDM Systems," *IEEE Transactions on Communications*, Vol. 52, No. 11, November 2004, pp. 1916-1926.
- [12] S. Sezginer and H. Sari, "Metric-Based Symbol Predistortion Techniques for Peak Power Reduction in OFDM Systems," *IEEE Transactions on Wireless Communications*, Vol. 6, No. 7, July 2007, pp. 2622-2629.
- [13] S. Yang and Y. Shin, "An Adaptive SLM Scheme Based on Peak Observation for PAPR Reduction of OFDM Signals," *IEICE Transactions on Fundamentals of Electronics, Communications and Computer Sciences*, Vol. E91, No. 1, January 2008, pp. 422-425.
- [14] A. D. S. Jayalath and C. Tellambura "SLM and PTS Peak-Power Reduction of OFDM Signals without Side Information," *IEEE Transactions on Wireless Communications*, Vol. 4, No. 5, September 2005. pp. 2006-2013.
- [15] C. L. Wang and S. J. Ku, "Novel Conversion Matrices for Simplifying the IFFT Computation of an SLM-Based PAPR Reduction Scheme for OFDM Systems," *IEEE Transactions on Communications*, Vol. 57, No. 7, July 2009, pp. 1903-1907.
- [16] L. Yanga, R. S. Chena, K. K. Soob and Y. M. Siub, "An Efficient Sphere Decoding Approach for PTS Assisted PAPR Reduction of OFDM Signals," *International Journal of Electronics and Communications*, Vol. 61, No. 10, November 2007, pp. 684-688.
- [17] Y. Zhang, Q. Ni and H.-H. Chen, "A New Partial Transmit Sequence Scheme Using Genetic Algorithm for Peak-to-Average Power Ratio Reduction in a Multi-Carrier Code Division Multiple Access Wireless System," *International Journal of Autonomous and Adaptive Communications Systems*, Vol. 2, No. 1, March 2009, pp. 40-57.
- [18] C. Tellambura, "Upper Bound on Peak Factor of N -multiple Carriers," *Electronic Letters*, Vol. 33, September 1997, pp. 1608-1609.
- [19] N. Y. Ermolova and P. Vainikainen, "On the Relationship between Peak Factor of a Multicarrier Signal and Aperiodic Autocorrelation of the Generating Sequence," *IEEE Communications Letters*, Vol. 7, No. 3, March 2003, pp. 107-108.
- [20] A. Ghassemi and T. A. Gulliver, "Low Autocorrelation Fractional PTS Subblocking for PAPR Reduction in OFDM Systems," *Proceedings of 6th Annual Conference on Communication Networks and Services Research*, Nova Scotia, May 2008, pp. 41-45.
- [21] C. Y. Hsu and H. Do, "The New Peak-to-Average Power Reduction Algorithm in the OFDM System," *Wireless Personal Communications*, Vol. 41, No. 4, June 2007, pp. 517-525.
- [22] E. Sun, K. Yi, B. Tian and X. Wang, "A Method for PAPR Reduction in MSE-OFDM Systems," *Proceedings of International Conference on Advanced Information Networking and Applications 2006*, Vienna, Vol. 2, April 2006, pp. 18-20.
- [23] D. Wu, S. Predrag and S. Ivan, "Ternary Complementary Sets for Multiple Channel DS-UWB with Reduced Peak-to-Average Power Ratio," *Proceedings of IEEE GLOBECO*, Texas, November 2004, pp. 3230-3234.
- [24] A. R. Ahmad, O. Basir and K. Hassanein, "An Intelligent Expert Systems Approach to Layout Decision Analysis and Design Under Uncertainty," Springer-Verlag, 2008, pp. 312-365.
- [25] A. R. Ahmad, "An Intelligent Expert System for Decision Analysis & Support," Ph.D. Thesis, University of Waterloo, Waterloo.
- [26] I. M. Hussain and I. A. Tasadduq, "PAPR Analysis in OFDM Signals Based on Power Variance," *Proceedings of Wireless Communications, Networking and Mobile Computing*, Dalian, October 2008, pp. 1-4.
- [27] M. Negnevitsky, "Artificial Intelligence: A Guide to Intelligent Systems," Pearson, Sydney, 2008.
- [28] A. V. Oppenheim and R. W. Schaffer, *Discrete-Time Signal Processing*, Englewood Cliffs: Prentice Hall, 1989.

Appendix

As indicated in (17), the normalized PV expression contains $N - 1$ AAC terms. AAC term can be represented by (12). In case of constant envelope mapper (e.g. QPSK which is used throughout our simulations), (12) can be modified into:

$$R_i = \sum_{k=0}^{N-1-i} \frac{d_k}{d_{k+i}}; \quad 0 \leq i \leq N-1$$

$$R_i = \left(\frac{d_0}{d_i} + \frac{d_1}{d_{i+1}} \right) + \left(\frac{d_2}{d_{i+2}} + \frac{d_3}{d_{i+3}} \right) + \dots + \frac{d_{N-i-1}}{d_{N-1}} \quad (22)$$

Hence each expression of R_i contains $N - i$ terms of kind (d_k / d_{k+i}) . Using (22) and (17) it can easily be shown that the total number of such terms in the power variance expression is $\sum_{i=1}^{N-1} N - i$. Similarly, the total number of pairs of adjacent terms in R_i as indicated by parenthesis in (22) is $N - i / 2$. Now one way to reduce AAC to their minimum values (i.e. 0 or 1 depending on i) is to make the summation of each and every pair of terms

in (22) equal to zero. Let $\left(\frac{d_p}{d_{p+i}} + \frac{d_{p+1}}{d_{p+i+1}} \right)$ be any pair in (22) where $p = 0, 2, 4, \dots, N - 2 - i$ (for even i) and $p = 0, 2, 4, \dots, N - 3 - i$ (for odd i). In case of $i = 1, 2, 3, \dots, N - 1$, to minimize the values of all such pairs to zero, we have to multiply every second complex number (i.e. subcarrier) starting from d_{p+i} by a factor $g_{i,v}$. This factor is obtained as shown below:

For the first $i / 2$ number of pairs:

$$\left(\frac{d_p}{g_{i,v} \times d_{p+i}} + \frac{d_{p+1}}{d_{p+i+1}} \right) = 0 \Rightarrow g_{i,v} = -\frac{d_p d_{p+1+i}}{d_{p+1} d_{p+i}}; \quad (23)$$

For rest of the pairs when i is even:

$$g_{i,v} = -\frac{\bar{d}_p d_{p+1+i}}{d_{p+1} d_{p+i}}; \quad (24)$$

For rest of the pairs when i is odd

$$g_{i,v} = -\frac{d_p d_{p+1+i}}{\bar{d}_{p+1} d_{p+i}}; \quad (25)$$

where

$$\bar{d}_p = d_p \times g_{i,v-i/2}, \bar{d}_{p+1} = d_{p+1} \times g_{i,v-i/2} \quad \text{and} \quad v = \frac{p}{2} + 1.$$

For example, in case of $N = 16$ subcarriers and $i = 4$, the fourth AAC becomes:

$$R_4 = \left(\frac{d_0}{d_4} + \frac{d_1}{d_5} \right) + \left(\frac{d_2}{d_6} + \frac{d_3}{d_7} \right) + \left(\frac{d_4}{d_8} + \frac{d_5}{d_9} \right) + \left(\frac{d_6}{d_{10}} + \frac{d_7}{d_{11}} \right) + \left(\frac{d_8}{d_{12}} + \frac{d_9}{d_{13}} \right) + \left(\frac{d_{10}}{d_{14}} + \frac{d_{11}}{d_{15}} \right)$$

This expression has 6 pairs i.e. $16 - 4 / 2$ and as many factors and each factor is used to minimize the corresponding pair to zero. Since i is even, then $p = 0, 2, 4, \dots, 10$.

For instance, the third pair in R_4 is $\left(\frac{d_4}{d_8} + \frac{d_5}{d_9} \right)$ where $v =$

3 and $p = 4$. In order to find the six factors used to minimize each pair, (23) is used for the first 2 pairs i.e.

$$g_{4,1} = -\frac{d_0 d_5}{d_1 d_4} \quad \text{and} \quad g_{4,2} = -\frac{d_2 d_7}{d_3 d_6}.$$

Rest of the factors are calculated using (24) as i is even. Hence,

$$g_{4,3} = -\frac{\bar{d}_4 d_9}{d_5 d_8}, \quad g_{4,4} = -\frac{\bar{d}_6 d_{11}}{d_7 d_{10}}, \quad g_{4,5} = -\frac{\bar{d}_8 d_{13}}{d_9 d_{11}} \quad \text{and}$$

$$g_{4,6} = -\frac{\bar{d}_{10} d_{15}}{d_9 d_{14}}, \quad \text{where} \quad \bar{d}_4 = d_4 \times g_{4,1}, \quad \bar{d}_6 = d_6 \times g_{4,2},$$

$$\bar{d}_8 = d_8 \times g_{4,3} \quad \text{and} \quad \bar{d}_{10} = d_{10} \times g_{4,4}.$$

Further, each alternate complex number starting from d_4 (i.e. $d_4, d_6, d_8, d_{12}, d_{14}, d_{16}$) will be multiplied by $g_{4,1}, g_{4,2}, g_{4,3}, g_{4,4}, g_{4,5}$ and $g_{4,6}$ respectively. In this manner $|R_4|$ will be minimized to zero. It is clear that \bar{d}_p or \bar{d}_{p+1} means that before minimizing the corresponding pair to zero, updation of d_p into \bar{d}_p has to take place first. In the above example, for the third pair, updation of d_4 (i.e. $\bar{d}_4 = d_4 \times g_{4,1}$) has to take place first after which minimization of that pair takes place. Thus, the third pair has the form $\left(\frac{\bar{d}_4}{d_8} + \frac{d_5}{d_9} \right)$

rather than $\left(\frac{d_4}{d_8} + \frac{d_5}{d_9} \right)$. Now in case of $i = 1$ i.e. R_1 which is an exception case, factor expression is given by (23) for the first pair and for the rest of the pairs, it is given by (24) where $\bar{d}_p = d_p \times g_{i,v-1}$. Further, each complex number starting from d_1 is going to be multiplied by the corresponding factor. In this manner, we can minimize the coefficients of any sequence to their respective minimum values using the procedure above.